EurJIC European Journal of Inorganic Chemistry
ChemPubSoc Europe
FULL PAPER

DOI:10.1002/ejic.201500029

Catalytic Models of Tyrosinase: Reactivity Differences between Systems Based on Mono- and Binucleating Ligands

Julia Schottenheim,[a] Claus Gernert,[b] Benjamin Herzigkeit,[a] Jan Krahmer,[a] and Felix Tuczek*[a]

Keywords: Bioinorganic chemistry / Metalloproteins / Enzyme models / Enzyme catalysis / Copper

A new tyrosinase model based on the binucleating ligand $L_{py}2$ is synthesized and characterized. The ligand $L_{py}2$ contains a combination of an imine and a pyridine function in the sidearms, which are bridged by a flexible alkyl spacer. As shown by UV/Vis and NMR spectroscopy, the $Cu_2L_{py}2$ complex catalyzed the conversion of the monophenol 2,4-di-*tert*-butylphenol (DTBP-H) into the *o*-quinone 3,5-di-*tert*-butylquinone (DTBQ) with a turnover number (TON) of 18. The dicopper complex of $L_{py}2$ thus shows monophenolase activity that is comparable to that of the recently developed $L_{py}1$ model of tyrosinase, which is based on a known mononucleating ligand (M. Rolff, J. Schottenheim, G. Peters, F. Tuczek, *Angew. Chem. Int. Ed.* **2010**, *122*, 6583). The electron-poor substrate 4-hydroxybenzoic acid methyl ester (MeBA-OH), in contrast, is converted by $Cu_2L_{py}2$ into the semiquinone. For both substrates, the oxygenation reactions were also conducted in a stoichiometric fashion to obtain information on the intermediates involved. For the substrate MeBA-OH, we detected a binuclear μ-catecholato copper(II) complex by high-resolution ESI mass spectrometry. These studies were complemented by investigations of deactivation mechanisms that could be invoked to explain the limitation of the TON. To this end, a bis-μ-hydroxido $L_{py}2$ dicopper(II) complex as well as a semiquinone $L_{py}2$ complex were prepared. Both complexes may represent decay products of the catalyst.

Introduction

Pigmentation is one of the most obvious phenotypic properties of living beings. It is based on melanin, which is one of the most common biopigments, and contributes to the richness of color in a variety of bacteria, fungi, plants, and animals. Melanins are heterogeneous polyphenolic biopolymers with a complex structure, the color of which varies from yellow to black.[1,2] The biosynthesis of melanin starts with conversion of the amino acid tyrosine into dopaquinone, which is catalyzed by tyrosinases.[2–4] Type 3 copper enzyme tyrosinase mediates the *o*-hydroxylation of monophenols to catechols and the subsequent two-electron oxidation to *o*-quinones (monophenolase activity, Scheme 1a),[5] but also shows diphenolase activity, which involves the two-electron oxidation of catechols to *o*-quinones (Scheme 1b).[6]

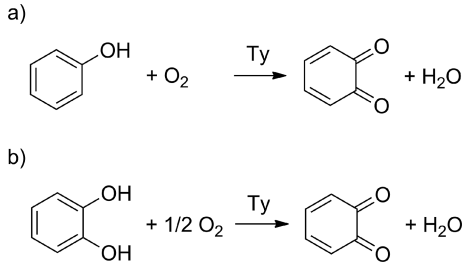

Scheme 1. (a) Monophenolase activity and (b) diphenolase activity of tyrosinase.

The first X-ray crystallographic characterization of a tyrosinase active site was performed for the bacterium *Streptomyces castaneoglobisporus*.[7] In analogy to the other two important Type 3 copper proteins hemocyanin and catechol oxidase, it contains a binuclear copper center, whereupon each copper is coordinated by three histidines. Bonding of dioxygen leads to the characteristic Cu_2 μ-η^2:η^2-peroxide structure,[8] which mediates the *o*-hydroxylation and two-electron oxidation of diphenolic substrates (see Scheme 2).

In 2009, the isolation and crystallization of a prophenol oxidase from the moth *Manduca sexta* was achieved, which is the inactive precursor of phenoloxidase in insects.[9] Since then more crystal structures of tyrosinase were obtained.[10]

[a] Institut für Anorganische Chemie, Christian-Albrechts-Universität zu Kiel,
Max-Eyth-Staße 2, 24118 Kiel, Germany
E-mail: ftuczek@ac.uni-kiel
http://www.ac.uni-kiel.de/tuczek
[b] Institut für Physikalische Chemie, Christian-Albrechts-Universität zu Kiel,
Max-Eyth-Staße 1, 24118 Kiel, Germany
Supporting information for this article is available on the WWW under http://dx.doi.org/10.1002/ejic.201500029.

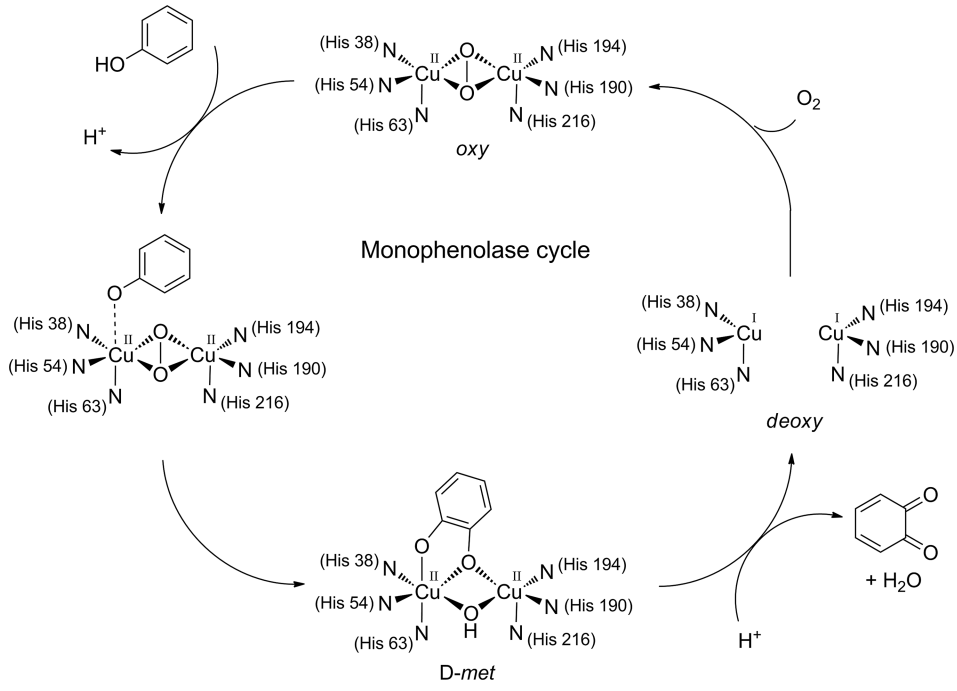

Scheme 2. Monophenolase cycle of tyrosinase.

The publications include the structures of enzymes from the fungus *Agaricus bisporus* and the bacterium *Bacillus megaterium*, and also studies with tyrosinase inhibitors.[10a,10b]

Numerous examples of small-molecule model systems reproducing the mono- and diphenolase activities of Type 3 copper proteins have been published.[11] However, the number of tyrosinase models exhibiting catalytic monophenolase remains very limited.[5] The first catalytic model systems of tyrosinase were based on binuclear copper complexes.[12–14] The functionalized sidearms in the ligands were bridged by comparatively rigid aromatic spacers such as xylyl for the L-66 system of Casella et al. or biphenyl for the BiPh(impy)$_2$ system of Réglier et al.[13,14] Bulkowski et al., in contrast, employed dicopper systems supported by macrocyclic ligands that contained flexible alkyl spacers.[12]

During the last few years, our group has synthesized a family of copper complexes based on mononucleating ligands that show catalytic monophenolase activity.[15–17] The ligands contain an imine function and a variable *N*-heterocyclic part, which was pyridine for $L_{py}1$, benzimidazole for $L_{bzm}1$, and pyrazole for $L_{hpz}1$ and $L_{hpz}2$ (Scheme 3a).

The copper(I) complex $[Cu^{I}L_{py}1(CH_3CN)_2]PF_6$ was shown to generate 3,5-di-*tert*-butylquinone (DTBQ) upon addition of 50 equiv. 2,4-di-*tert*-butylphenol (DTBP-H), 100 equiv. NEt_3 and molecular oxygen with a turnover number (TON) of 18 after 8 hours.[15] By replacing the pyridine function with benzimidazole ($L_{bzm}1$) or pyrazole ($L_{hpz}1$, $L_{hpz}2$) (Scheme 3a), both the reaction rate and turnover number of the catalytic conversion of monophenol DTBP-H into the *o*-quinone DTBQ could be increased.[15–17] The highest TON of 31 was achieved by catalytic oxygenation of a 500 μM solution of $[Cu^{I}L_{bzm}1$-

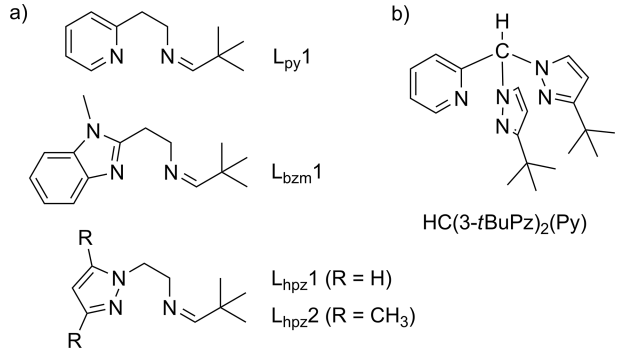

Scheme 3. Mononucleating ligands for model complexes: (a) $L_{py}1$, $L_{bzm}1$, $L_{hpz}1$, and $L_{hpz}2$ developed by our research group, and (b) the HC(3-*t*BuPz)$_2$(Py) ligand of Herres-Pawlis et al.

$(CH_3CN)_2]PF_6$ in dichloromethane after 6.5 hours.[16] In the meantime, another catalytic model was published that was based on a mononucleating ligand. The HC(3-*t*BuPz)$_2$-(Py) ligand developed by Herres-Pawlis, Stack et al. contains pyridine and pyrazole functions (Scheme 3b). The derived copper(I) complex forms a stable dioxygen adduct and exhibits catalytic monophenolase activity toward a variety of monophenolic substrates.[18]

In this paper, we combine a flexible alkyl spacer with pyridine-imine-functionalized sidearms to obtain a new binucleating ligand, $L_{py}2$ (Scheme 4). The bridging of the sidearms should mainly contribute to stabilize the intermediates of the catalytic cycle. In particular, we wanted to further characterize the catecholato species that is comparable to the D-*met* form of the enzymatic system (Scheme 2). Moreover, the performance of the $L_{py}2$ system with respect to the catalytic conversion of monophenols

into *o*-quinones has been determined. Regarding this activity, it is of interest to evaluate the influence of the bridge, which is present in $L_{py}2$ and absent in $L_{py}1$. Furthermore, the activity of the $L_{py}2$ system with respect to an electron-rich (DTBP-H) and an electron-poor substrate 4-hydroxybenzoic acid methyl ester (MeBA-OH) were compared. Finally, studies on the deactivation of the catalyst complexes were conducted to understand the limitation of the turnover number of the models.

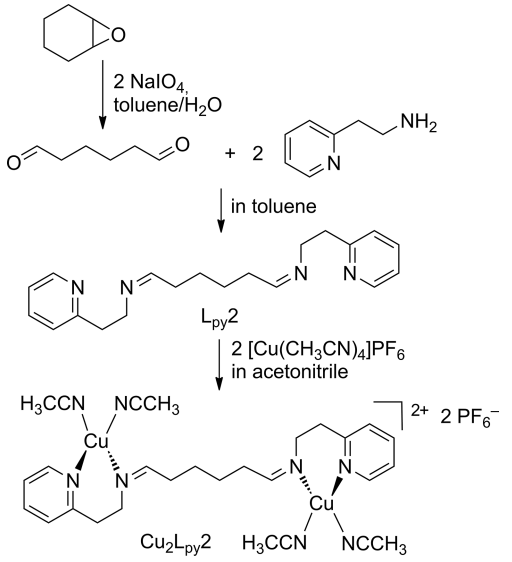

Scheme 4. Synthesis of ligand $L_{py}2$ and the corresponding copper(I) complex $Cu_2L_{py}2$.

Results and Discussion

Synthesis of the Ligand $L_{py}2$ and the Copper(I) Complex $Cu_2L_{py}2$

The synthesis of $L_{py}2$ (Scheme 4) started with oxidative ring opening of cylohexene oxide to give hexane-1,6-dial.[19]

The imine condensation of 2-(pyrid-2-yl)ethylamine (2 equiv.) and hexane-1,6-dial provided $L_{py}2$, which was converted into the corresponding copper(I) complex $Cu_2L_{py}2$ by addition of tetrakis(acetonitrile)copper(I) hexafluorophosphate (2 equiv.) under anaerobic conditions. All compounds were obtained in satisfactory yields and purities (see Exp. Sect.).

Catalytic Monophenolase Activity of the $L_{py}2$ Model System

To test the catalytic activity of the new model system involving $L_{py}2$, a catalytic oxygenation was performed and monitored by in situ UV/Vis spectroscopy at room temperature. A mixture of DTBP-H (100 equiv.) and triethylamine (200 equiv.) was added to a solution of $Cu_2L_{py}2$ (500 μM) in dichloromethane under anaerobic conditions, then molecular oxygen was bubbled through the solution. The $L_{py}2$ system catalytically generated DTBQ, which was detected by the evolution of the 407 nm absorption band (Figure 1).

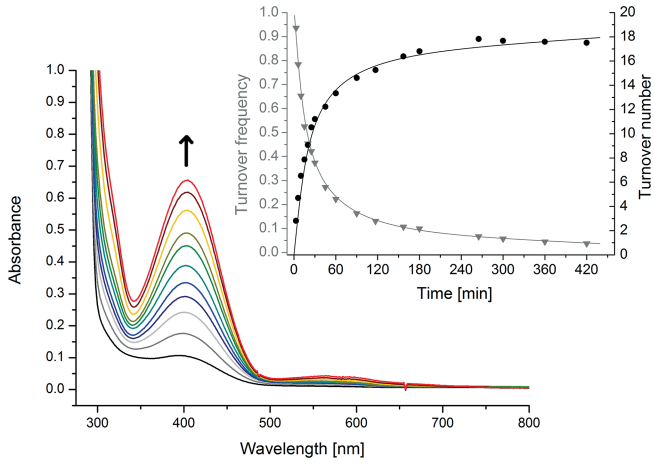

Figure 1. Catalytic oxygenation of a 500 μM solution of $Cu_2L_{py}2$ in dichloromethane in the presence of DTBP-H (100 equiv.) and NEt_3 (200 equiv.) during the first 3 h at room temperature. The solution was diluted before each measurement to a concentration of 200 μM of $Cu_2L_{py}2$; l = 1 mm. (Inset) Turnover number per dicopper unit (black circle) and turnover frequency per minute (gray triangle) as a function of time over 7 h of oxygenation.

Based on an ε-value of 1830 $L\,mol^{-1}\,cm^{-1}$, the system produces 16 TON per dicopper unit during the first 3 h.[13] The rate of DTBQ formation decreases with time and, after 4.5 h, the yield reaches a maximum value of 18 turnovers (Figure 1 inset).

During the first 5 min of oxygenation, the turnover frequency (TOF) was approximately 0.8 turnovers per minute and this was halved within 30 min. With further reaction time, the TOF decreases continuously until it becomes almost zero after 7 h (Figure 1 inset).

The $Cu_2L_{py}2$ complex is thus able to catalytically mediate the conversion of monophenol DTBP-H into *o*-quinone DTBQ with a TON that is comparable to that of the $L_{py}1$ system.[15,16] The bridging of the pyridine-imine units by the flexible alkyl chain of the $L_{py}2$ system therefore does not hinder the catalytic monophenolase activity. On the contrary, the $L_{py}2$ system is faster at the beginning of oxygenation than its $L_{py}1$ counterpart, and it remains stable for longer after reaching the maximum TON (see below).

After 1 h of oxygenation, a small portion of the reaction mixture was diluted to a concentration of 25 μM $Cu_2L_{py}2$ in dichloromethane. This solution was treated with 6 M hydrochloric acid and extracted with dichloromethane to eliminate any copper species. The solvent was removed under reduced pressure and the resulting residue was investigated by ^1H NMR spectroscopy (Figure 2).

Integration of the respective signals in the ^1H NMR spectrum (Figure 2) showed that after 1 h of oxygenation, 77% of the starting amount of DTBP-H remained, 9% was converted into the C–C coupling product 3,3′,5,5′-tetra-*tert*-butyl-2,2′-biphenol,[20,21] and 14% of DTBP-H was converted into *o*-quinone DTBQ, in accordance with the TON of 14 determined spectrophotometrically after that reaction time.

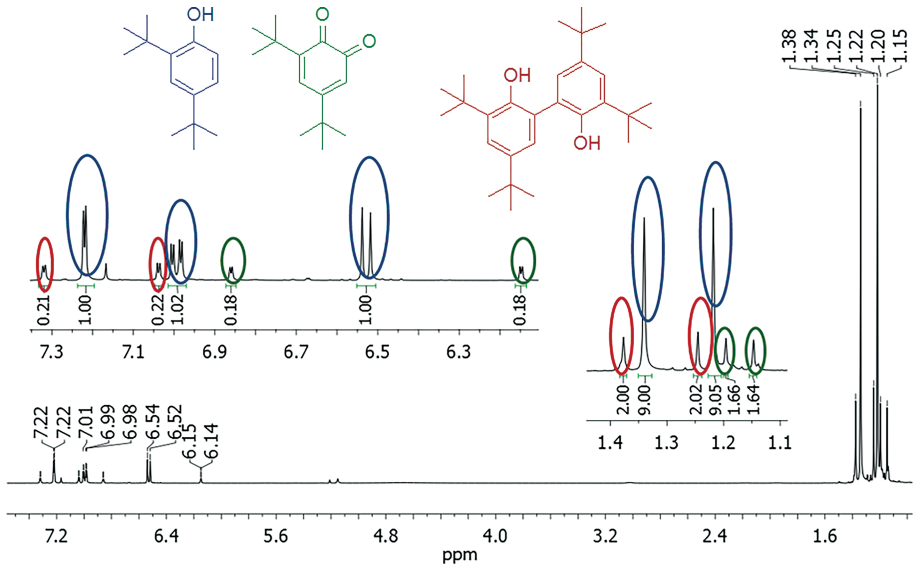

Figure 2. ^{1}H NMR spectrum of the organic phase after HCl quench (1 h oxygenation) with detected compounds (blue: DTBP-H, green: DTBQ; red: C–C coupling product).

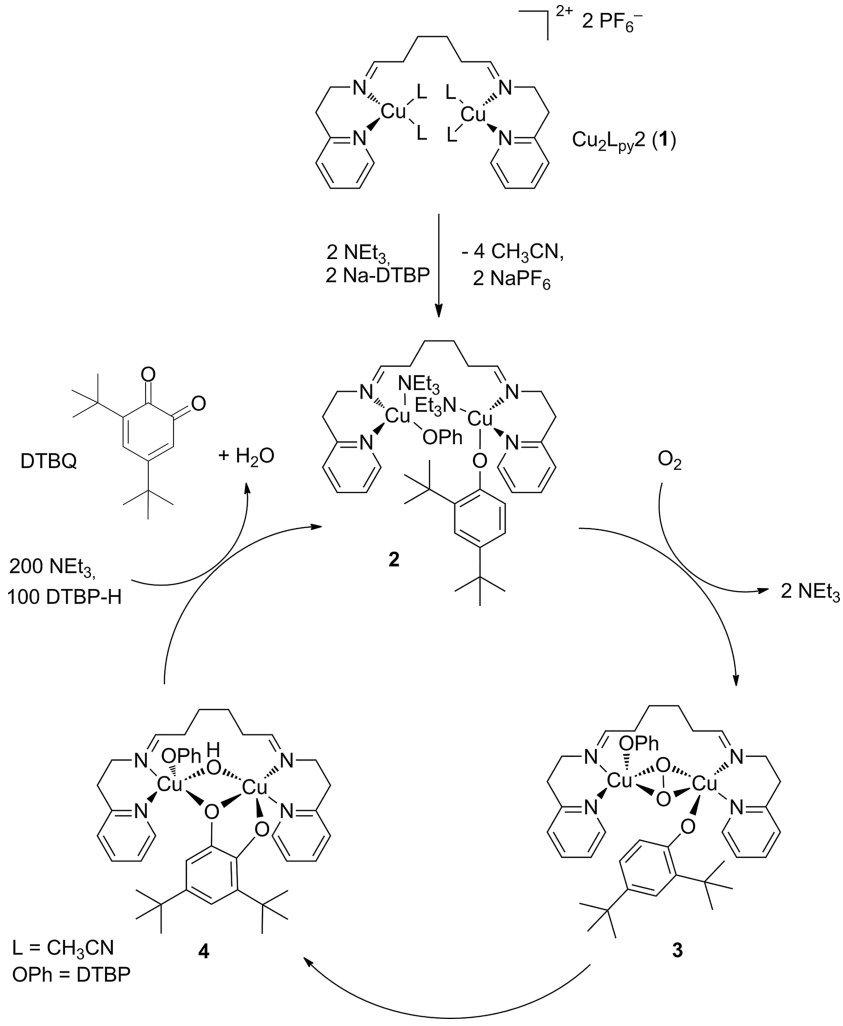

Scheme 5. Proposed mechanistic cycle of the $L_{py}2$ model system.

In comparison to the mononuclear models ($L_{py}1$, $L_{bzm}1$), the formation of the C–C coupling product, and thus the unwanted free-radical side reaction, could be significantly reduced in the $L_{py}2$ system. After 1 h of catalytic oxygenation, only 9% of the coupling product was found; at that reaction time, 22% of coupling product was produced by the $L_{py}1$ and even 47% by the $L_{bzm}1$ system.[15,16] Suppression of the free-radical side reaction may be attributed to better shielding of the peroxide moiety in the side-on-peroxo intermediate (see Scheme 5) through the alkyl-bridged ligand $L_{py}2$. This shielding, in particular, prevents the H-atom abstraction reaction of phenols leading to phenoxyl radicals, which represents the initial step of the free-radical pathway.[20,21] In addition, steric factors may prevent the recombination of two phenoxyl radicals, leading to the C–C coupling product.

Catalytic Oxygenation of the Substrate MeBA-OH

The catalytic oxygenation was also carried out by using the substrate MeBA-OH, which has an electron-withdrawing methyl ester function instead of the electron-donating *tert*-butyl groups. A mixture of MeBA-OH (100 equiv.) and triethylamine (200 equiv.) was added to a 250 μM solution of $Cu_2L_{py}2$ in dichloromethane under anaerobic conditions, then molecular oxygen was bubbled through the solution for 5 h. The resulting UV/Vis spectra are shown in Figure 3.

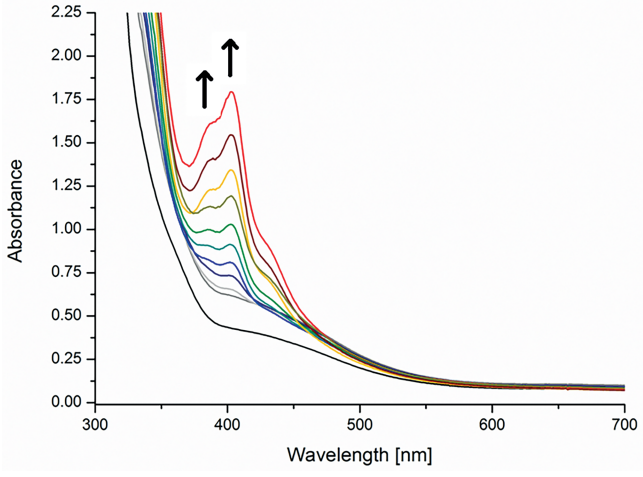

Figure 3. Catalytic oxygenation of a 250 μM solution of $Cu_2L_{py}2$ in dichloromethane in the presence of MeBA-OH (100 equiv.) and NEt_3 (200 equiv.) during the first 5 h at room temperature; l = 1 mm.

The spectra differ greatly from those of the catalytic oxygenation of the electron-rich substrate DTBP-H. In particular, they show a peak at 402 nm and two shoulders at 385 and 430 nm, indicating the formation of semiquinones.[23,24] Given that semiquinones have extinction coefficients of approximately 7500 $L\,mol^{-1}\,cm^{-1}$,[24] the $L_{py}2$ system was calculated to generate MeBASQ catalytically in nine turnovers per dicopper unit after 5 h.

Clearly, the electron-withdrawing effect of the methyl ester group in the substrate MeBA-OH hinders its complete oxidation to the *o*-quinone. Therefore, only the semiquinone MeBASQ is generated, which presumably is formed by one-electron oxidation of the catechol resulting from the *o*-hydroxylation of MeBA-OH. We assume that in the catalytic formation of the semiquinone MeBASQ (analogous to Scheme 5), the semiquinone is released from intermediate **4** by one-electron oxidation of the catechol. The resulting mixed-valent Cu^I–Cu^{II} complex is reduced to the Cu^I–Cu^I form by one-electron reduction from the "phenol pool" of the reaction mixture.

Stepwise Performance of the Catalytic Cycle for the $L_{py}2$ Model System

Due to the close analogy to the $L_{py}1$ system, we propose the mechanistic cycle shown in Scheme 5 for the new $L_{py}2$ model of tyrosinase. To confirm this mechanistic cycle, a stoichiometric oxygenation was performed with the standard substrate DTBP-H. The resulting absorption spectra were very similar to those obtained by stoichiometric oxygenation of DTBP-H with the $L_{py}1$ system (Figure 4).[15]

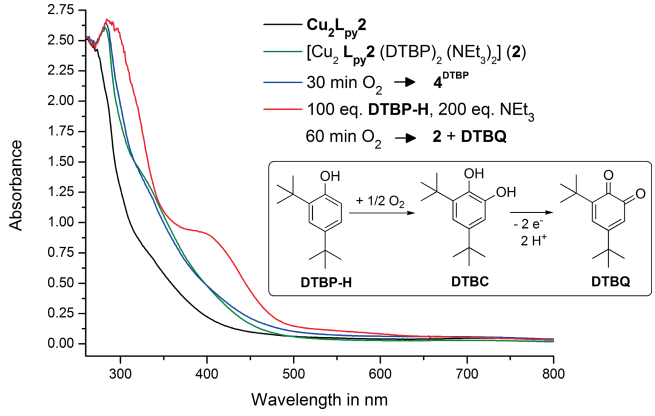

Figure 4. Stoichiometric oxygenation of a 250 μM solution of $Cu_2L_{py}2$ in dichloromethane with the substrate DTBP-H; l = 10 mm.

At first a 250 μM solution of $Cu_2L_{py}2$ was prepared under a nitrogen atmosphere and the UV/Vis spectrum was measured. This is the precursor **1** of the catalytically active species **2** (cf. Scheme 5), and does not exhibit significant absorbance in the visible region (Figure 4, black line). In the next step, the phenolato complex $[Cu^I_2L_{py}2(DTBP)_2(NEt_3)_2]$ (**2**) is prepared by reaction of $Cu_2L_{py}2$ with sodium-2,4-di-*tert*-butylphenolate (Na-DTBP; 2 equiv.) and NEt_3 (2 equiv.) in dichloromethane under Schlenk conditions.

In addition, we were able to synthesize the phenolato copper(I) complex **2** directly and characterized it by NMR spectroscopy (see Exp. Sect.). The corresponding absorption spectrum (Figure 4, green line) clearly shows a shoulder at approximately 330 nm, which can be associated with a phenolate-to-copper(I) ligand-to-metal charge transfer

(LMCT) transition.[25,26] While molecular oxygen is introduced into the reaction mixture of the stoichiometric oxygenation for 30 min, the absorbance at 330 nm decreases (Figure 4, blue line) and the color of the solution changes from yellow to brown. In case of the $CuL_{py}1$ system, the formation of a μ-catecholato complex $\mathbf{4}^{py}$ ("compound **4**") could be evidenced at this stage of the reactive cycle.[15,16] We assume that an analogous intermediate, $\mathbf{4}^{DTBP}$, is formed in case of the $Cu_2L_{py}2$ system, which should have a higher stability because of the alkyl spacer. However, the change in the absorption spectrum is rather insignificant (Figure 4, blue line).

Subsequently, catalytic conditions were re-established by addition of DTBP-H (100 equiv.) and NEt_3 (200 equiv.), followed by further oxygenation for 60 min. The resulting spectrum (Figure 4, red line) shows the known absorbance at 407 nm, which is caused by DTBQ. The catalytic oxygenation can be continued for a few hours with a steady increase of the band at 407 nm. After 2 h, three turnovers of DTBQ were generated. This shows that the catecholato intermediate **4** is also catalytically competent, although to a lesser degree than the copper(I) complex **2**, which produces 16 turnovers under comparable conditions (see Figure 1).

Unfortunately, no direct observation of a peroxo adduct was possible in our system. With respect to this point, it is known that binuclear copper(I) complexes supported by binucleating ligands containing flexible alkyl spacers also form intermolecular peroxo species.[22] To address this point, kinetic measurements were carried out by varying the concentration of the catalyst (see Exp. Sect.). From the fact that the rate of product formation scales linearly with the concentration of the binuclear copper(I) precursor $Cu_2L_{py}2$ (see the Supporting Information, Figure S1), we conclude that dioxygen predominantly binds in an intramolecular fashion and that the side-on-peroxo intermediate **3**, shown in Scheme 5, is in fact the catalytically active species.

A stoichiometric oxygenation reaction was also performed by using the substrate MeBA-OH, which has an electron-withdrawing methyl ester function instead of the electron-donating *tert*-butyl groups of DTBP-H. The electron-withdrawing effect hinders the oxidation of bound catecholate to *o*-quinone (see above) and thus should contribute to a further stabilization of the catecholato species $\mathbf{4}^{MeBA}$.[26]

The stoichiometric oxygenation with MeBA-OH was monitored by UV/Vis analysis, and the results are shown in Figure 5. A 250 μM solution of $Cu_2L_{py}2$ was prepared under a nitrogen atmosphere and the corresponding UV/Vis spectrum is given by the black line. The phenolato species $[Cu^{I}_2L_{py}2(MeBA\text{-}O)_2(NEt_3)_2]$ (**2**) was generated by adding MeBA-OH (2 equiv.) and NEt_3 (4 equiv.). The spectrum exhibits a strong absorption at approximately 310 nm, which can be attributed to a phenolate-to-copper(I) LMCT transition (Figure 5, green line).[25,26] While molecular oxygen is introduced into the solution for 30 min, the catecholato copper(II) intermediate $\mathbf{4}^{MeBA}$ is formed, as evident from an increase of the absorbance at 340 nm and the appearance of a shoulder at 430 nm.[27,28] This spectrum is in agreement with the features of the catecholato species of the Cu_2L-66 system.[26]

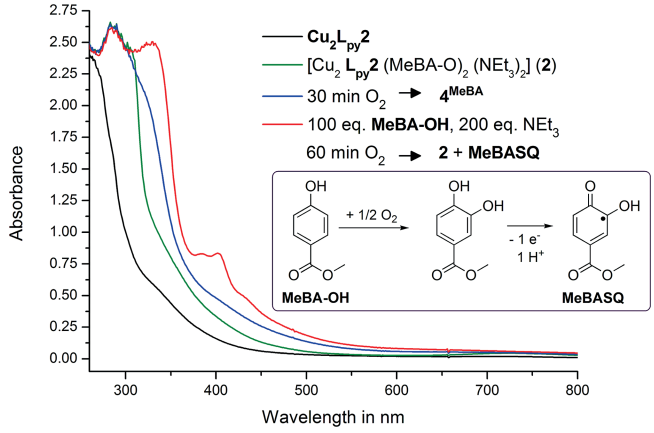

Figure 5. Stoichiometric oxygenation of a 250 μM solution of $Cu_2L_{py}2$ in dichloromethane with the substrate MeBA-OH; l = 10 mm.

After addition of MeBA-OH (100 equiv.) and NEt_3 (200 equiv.) and oxygenation for another 60 min, the spectrum shown in Figure 5 (red line) was obtained. Importantly, the spectrum shows a peak at 402 nm and two shoulders at 385 and 430 nm, which indicates the formation of semiquinone.[23,24]

Direct catalytic oxygenation of a mixture of $Cu_2L_{py}2$, MeBA-OH (100 equiv.) and triethylamine (200 equiv.) in dichloromethane generated the same spectrum (see Figure 3). This confirms that with the electron-poor substrate MeBA-OH, the *o*-quinone cannot be formed and only the semiquinone MeBASQ is generated. This final product evidently results from one-electron oxidation of the catecholato intermediate formed by *o*-hydroxylation of MeBA-OH (see Figure 5).

Catecholato Intermediates $\mathbf{4}^{DTBP}$ and $\mathbf{4}^{MeBA}$

The spectroscopic changes that occurred during the stoichiometric oxygenation with MeBA-OH suggest a sufficient stability of the corresponding catecholato intermediate **4** in the $L_{py}2$ system to allow its direct synthesis and isolation.

In fact, we succeeded in preparing the catecholato intermediate $\mathbf{4}^{MeBA}$ by the following route. A solution of $Cu_2L_{py}2$ (31.6 mg, 35.0 μmol) in dichloromethane (3 mL) was prepared under Schlenk conditions. A solution of MeBA-OH (10.7 mg, 70.0 μmol) and NEt_3 (14.2 mg, 140 μmol) in dichloromethane (3 mL) was added slowly. Molecular oxygen was introduced into the solution for 30 min, which changed the color from light-brown to dark-green. After the oxygenation the reaction mixture was overlaid with diethyl ether (20 mL) and it was allowed to stand for 30 min at room temperature. The solution was decanted from the precipitated gray-green solid, which was dried in air for 1 d to yield intermediate $\mathbf{4}^{MeBA}$ (19 mg, 70%) as a gray-green solid.

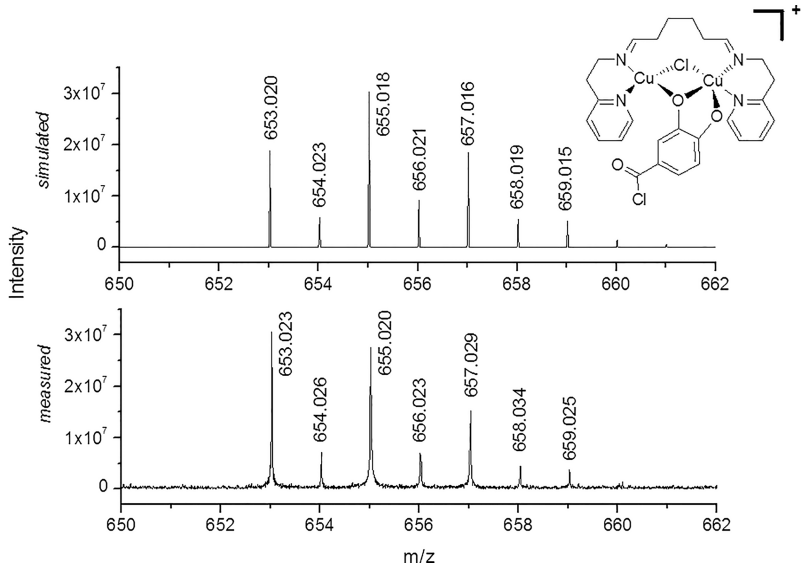

Figure 6. Segment of the HRMS (ESI) of $\mathbf{4}^{MeBA}$: simulated and measured isotope pattern of the complex $[M + 2Cl - OH - OCH_3]^+$ as shown top right.

The reaction product could be characterized as a solid with UV/Vis spectroscopy (see the Supporting Information, Figure S2) and by high-resolution ESI mass spectrometry (for the full spectrum see the Supporting Information, Figure S3). The simulated and measured isotope patterns correspond to $\mathbf{4}^{MeBA}$ in the form of $[M + 2Cl - OH - OCH_3]^+$ (Figure 6). This is the complete binuclear copper(II) complex with a coordinated catecholate. However, an exchange of hydroxide and methoxide with chloride occurred during the measurement, for which dichloromethane was used as solvent. Specifically, the bridging OH ligand was replaced by a μ-chlorido ligand and the OCH_3-group of the methyl ester function of the catecholate was substituted by chloride (see Figure 6 and Scheme 6). {HRMS (ESI; CH_2Cl_2, CH_3OH): m/z = 653.023 $[M + 2Cl - OH - OCH_3]^+$; calcd for $C_{27}H_{29}Cl_2Cu_2N_4O_3$: m/z = 635.020}.

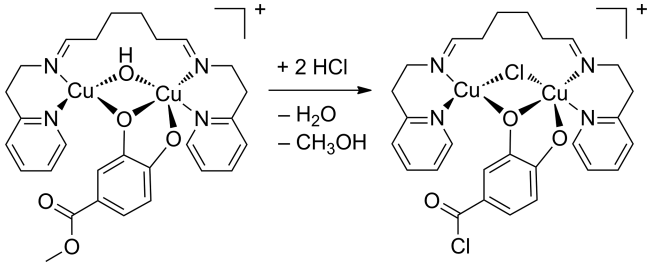

Scheme 6. Formation of the complex $[M + 2Cl - OH - OCH_3]^+$ during the MS (ESI) measurements of the intermediate $\mathbf{4}^{MeBA}$; HCl derives from the solvent dichloromethane.

Isolation and mass-spectrometric investigation of the catecholato adduct was also performed for the electron-rich substrate DTBP-H. However, in this case, the MS data were less clear.

To further confirm that both substrates (DTBP-H and MeBA-OH) are coordinated as catecholate in the respective intermediates **4**, HCl quenching was performed by using 250 μM solutions of $\mathbf{4}^{DTBP}$ and $\mathbf{4}^{MeBA}$, respectively, in CH_2Cl_2 (Figure 7). The spectra before the quenches show

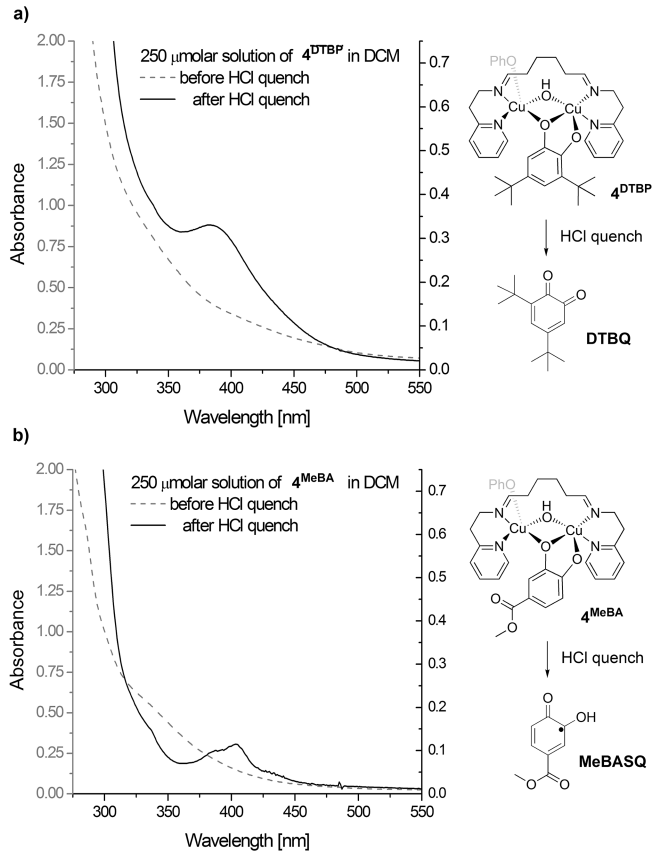

Figure 7. UV/Vis spectra of the intermediates (a) $\mathbf{4}^{DTBP}$ and (b) $\mathbf{4}^{MeBA}$ in dichloromethane before and after HCl quench (l = 10 mm); OPh = DTBP (a) and MeBA-O (b). Left scales refer to the initial, right scales refer to the final spectra.

the known absorption bands of the catecholato species (cf. Figures 4 and 5, blue lines). After quenching, the characteristic absorbances of DTBQ (407 nm) or semiquinone MeBASQ were detected (see Figure 7).[23,24] By addition of HCl, coordinated 3,5-di-*tert*-butyl catecholate (DTBC) is therefore released as *o*-quinone DTBQ, whereas in the case of MeBA-OH, only the semiquinone is formed.

Deactivation of the Catalytically Active Complex

Deactivation of the catalytic system is evident, inter alia, from an intense blue coloration of the oxygenation mixture, which occurs in the $L_{py}1$ and $L_{bzm}1$ systems already after 15 h but for the $L_{py}2$ model is only clearly visible after two days. With respect to the formation of this decay product, the $L_{py}2$ system thus appears to be more stable than its $L_{py}1$ counterpart. The blue species shows a strong absorbance at 589 nm with an ε-value of approximately 1000 $L\,mol^{-1}\,cm^{-1}$ (see the Supporting Information, Figure S4).

The blue coloration of the reaction mixture and the deactivation of the catalytically active complex go hand in hand. To obtain more information about these processes, two possible inactive complexes that could be formed in the oxygenation mixture were explored. One possibility is the formation of a stable bis-μ-hydroxido dicopper(II) complex through reaction with water, which accumulates in solution as the oxygenation proceeds (see Scheme 7). It was possible

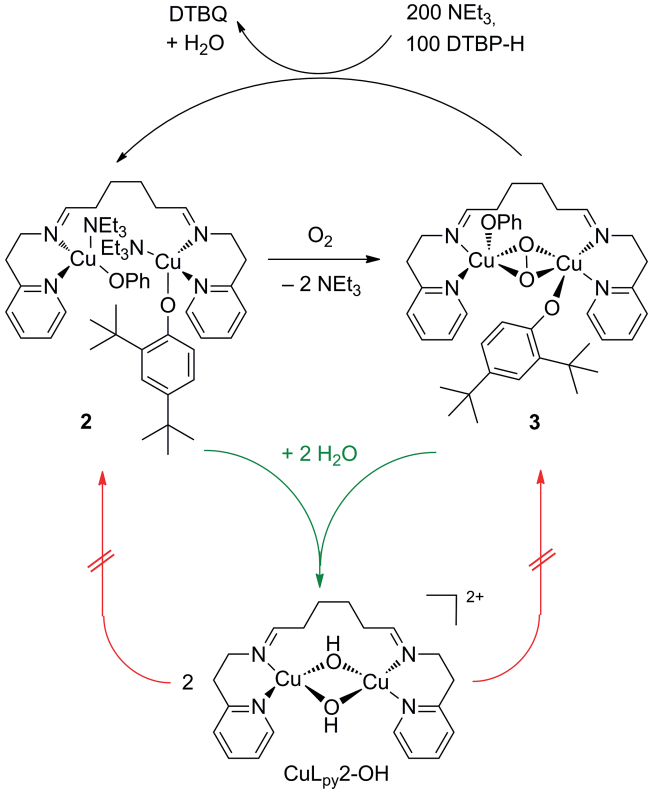

Scheme 7. Influence of water on the catalytic cycle and formation of the inactive $CuL_{py}2$-OH complex during oxygenation.

to synthesize the bis-μ-hydroxido-copper(II) complex $CuL_{py}2$-OH independently (see Exp. Sect.)[29] and characterize it by HRMS (ESI) analysis (for the full spectrum see the Supporting Information, Figure S5). The simulated and measured isotope patterns show very good agreement (Figure 8).

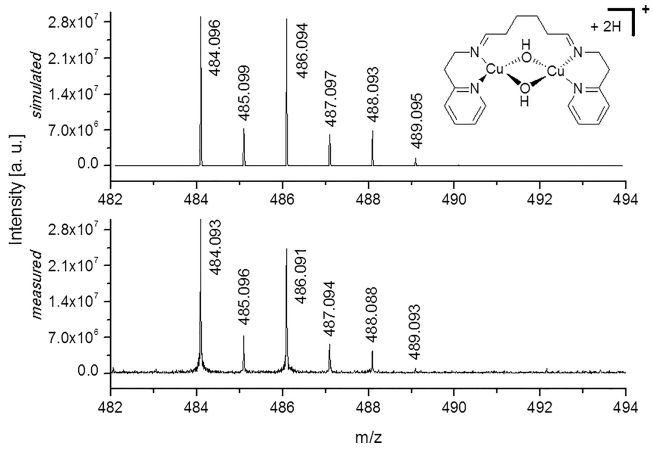

Figure 8. Segment of the HRMS (ESI) of $CuL_{py}2$-OH: simulated and measured isotope pattern of the complex $[M + 2H]^+$ as shown top right.

Solutions with different concentrations of the complex $CuL_{py}2$-OH in acetone were prepared and UV/Vis spectra were measured (see the Supporting Information, Figure S6). They show an absorption at 611 nm, but with an extinction coefficient (ε = 72 $L\,mol^{-1}\,cm^{-1}$) that is too small in comparison with the blue species. Nevertheless, the bis-μ-hydroxido-copper(II) complex $CuL_{py}2$-OH could be detected by ESI mass spectrometry in the blue oxygenation mixture of the catalytic oxygenation after two days.

The other possible deactivation scenario involves the formation of a copper(II) semiquinone complex. It is known that *o*-quinones and, especially, DTBQ form these complexes in the presence of copper(I) species and chelate ligands.[30–34] We were able to generate a blue semiquinone copper(II) complex with the binucleating ligand $L_{py}2$ directly in solution and detect it in situ by UV/Vis spectroscopy. For this experiment, a solution of $Cu_2L_{py}2$ (5 mM, 13.6 mg, 15.0 μmol) in tetrahydrofuran (3 mL) was prepared under anaerobic conditions. Upon addition of DTBQ (6.60 mg, 30.0 μmol), the light-yellow solution immediately became dark-blue. The solution was diluted to record UV/Vis spectra (see the Supporting Information, Figure S7). They show an intense absorption at 736 nm with an extinction coefficient of ε = 1255 $L\,mol^{-1}\,cm^{-1}$ that is comparable to the ε-value of the blue species. However, the wavelength of the absorption band is more than 100 nm too high. The oxygenation mixture contains many species that may act as additional ligands to further stabilize a copper(II) semiquinone complex. At present, we cannot determine the exact identity of the copper(II) semiquinone complex, but the above experiment shows that its formation is possible under the respective conditions and, in fact, may

cause the intense blue coloration of the reaction mixture after long reaction times.[30]

Conclusions

Based on the binucleating ligand $L_{py}2$, the synthesis of a new model system of tyrosinase has been achieved. Catalytic oxygenation of DTBP-H is mediated with a turnover number that is similar to that obtained with the mononuclear $L_{py}1$ model (Scheme 8).[15,16] Bridging of the pyridine-imine units by the flexible alkyl chain therefore does not hinder the catalytic monophenolase activity. On the contrary, the $L_{py}2$ system is faster at the beginning of oxygenation than its $L_{py}1$ counterpart, and the unphysiological free-radical side-reaction, which leads to the biphenolic C–C coupling product, is significantly reduced.

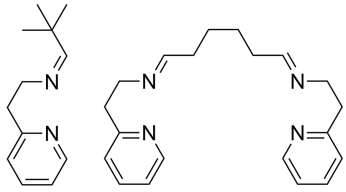

System	$L_{py}1$	$L_{py}2$
TON	*22*	*18*
TOF (5 min)	0.56	0.82
TOF (60 min)	0.24	0.23
C-C coupling product (60 min)	22%	9%

Scheme 8. Comparison of the $L_{py}1$ und $L_{py}2$ systems.

Besides the standard substrate DTBP-H, it was also possible to catalytically oxygenate the electron-poor substrate MeBA-OH by using the $L_{py}2$ system. In this case, however, the corresponding semiquinone MeBASQ is obtained.

The bridging alkyl spacer stabilizes the intermediates without changing the mechanism. In this respect, the $L_{py}1$ and $L_{py}2$ pair of ligand systems corresponds to, for example, the L-6 and L-66 ligands of Casella and coworkers.[35] As for the $L_{py}1$ system, the relevant intermediates of the $L_{py}2$ catalytic cycle could be generated in a stepwise fashion and detected by UV/Vis spectroscopy, showing defined spectral changes, especially when using MeBA-OH as substrate. Moreover, the copper(I) phenolato intermediates **2** were characterized by NMR spectroscopy, and the catecholato intermediate $\mathbf{4}^{MeBA}$ was detected by high-resolution ESI mass spectrometry. Unfortunately, we were unable to detect the side-on-peroxo bridged intermediates **3**, also at low temperatures, but it could be shown by means of kinetic experiments that no intermolecular peroxo species are formed.

By HCl quenching, the bound catecholates of compounds $\mathbf{4}^{DTBP}$ and $\mathbf{4}^{MeBA}$ could be released, leading to quinone for the electron-rich substrate DTBP-H and semiquinone for the electron-poor substrate MeBA-OH.

These studies were complemented by investigations of the deactivation mechanisms of the employed catalyst to explain the limitation of the TON. In this regard, we were able to obtain a high-resolution ESI mass spectrum of the $L_{py}2$ bis-μ-hydroxido copper(II) complex, which may be one of the dead-end species of the catalytic system. Another possibility is the formation of a copper(II) semiquinone complex, which accounts for the intense-blue coloration of the reaction mixture after prolonged reaction times. With respect to this deactivation mechanism, the $L_{py}2$ system appears to be more stable than its $L_{py}1$ analogue, although this apparently does not lead to a higher turnover number.

Experimental Section

Materials and Techniques: All reagents were used as received from Sigma–Aldrich and Abcr GmbH & Co. KG. Solvents were all used as reagent grades. Dichloromethane, toluene, and acetonitrile were purified further by heating to reflux over calcium hydride and distilled under nitrogen atmosphere. Diethyl ether and tetrahydrofuran were purified by heating to reflux over lithium-aluminum hydride and methanol over magnesium methoxide and distilled under nitrogen atmosphere. Elemental analyses were performed with a Euro Vector CHNS-O-element analyzer (Euro EA 3000) and the samples were burned in sealed tin containers in an oxygen stream. The content of chloride was determined according to Schöniger[36] with a potentiograph E536 from Metrohm using ion selective electrodes. The NMR spectra were recorded at 300 K with a Bruker Avance 400 Pulse Fourier Transform spectrometer operating at a ^{1}H frequency of 400.13 MHz and a ^{13}C frequency of 100.62 MHz and were referenced on residual protons of the solvent. Optical absorption spectra were recorded in solution with an Agilent Technologies 8453 UV/Vis spectrophotometer (l = 1 mm and l = 10 mm). High-resolution (ESI) mass spectra were measured with an APEX 3 FT-ICR mass spectrometer from Bruker Daltonics (7.05 T magnet).

Hexane-1,6-dial: A suspension of sodium periodates (1.50 g, 7.01 mmol) in a mixture of toluene (60 mL) and distilled water (8 mL) was stirred for 15 min at room temperature. Cyclohexene oxide (310 mg, 3.16 mmol) was added and the reaction mixture was stirred for 4 d at room temperature. The resulting solid was filtered off and the solution was allowed to stand for 2 d. The formed solid was filtered off again, the phases were separated, and the aqueous phase was extracted with toluene (2 × 20 mL). The combined organic phases were washed with distilled water (20 mL) and with brine (20 mL). After drying over magnesium sulfate, the solvents were removed under reduced pressure to give a light-yellow oil, which crystallized after a few weeks to a colorless solid, yield 103 mg (29%); ^{1}H NMR (400 MHz, $CDCl_3$): δ = 9.73 (t, 2 H, -CHO), 2.44 (m, 4 H, CH_2CHO), 1.62 (m, 4 H, CH_2CH_2CHO) ppm. ^{13}C NMR (100 MHz, $CDCl_3$): δ = 201.84 (CH, 2 C, CHO), 43.53 (CH_2, 2 C, CH_2CHO), 21.46 (CH_2, 2 C, CH_2CH_2CHO) ppm; $C_6H_{10}O_2$ (114.14): calcd. C 63.14, 8.83, 0.00; found C 63.75, H 8.65, N 0.00.

1,6-Bis[(2-pyrid-2-yl)iminoethylene]hexane ($L_{py}2$): Hexane-1,6-dial (172 mg, 1.51 mmol) was filled into a Schlenk flask fitted with a Dean–Stark trap and flushed with nitrogen for 30 min. The aldehyde was diluted in anhydrous toluene (40 mL) and 2-(pyrid-2-yl)ethylamine (573 mg, 4.69 mmol) was added dropwise. The mixture was stirred and heated to reflux with removal of water for 6 h. After cooling to room temperature, the solution was decanted

from the residue, which was discarded. The solvent was removed immediately under reduced pressure to obtain a dark brown oil, yield 475 mg (97%). ^{1}H NMR (400 MHz, $CDCl_3$): δ = 8.46 (dq, 2 H, Py H-6), 7.53 (td, 2 H, Py H-4), 7.10–7.04 (m, 6 H, imine H, Py H-3, Py H-5), 3.05 (t, 4 H, Py-CH_2-CH_2), 2.86 (t, 4 H, Py-CH_2), 2.04 (m, 4 H, imine-CH_2), 1.18 (m, 4 H, imine-CH_2-CH_2) ppm. ^{13}C NMR (100 MHz, $CDCl_3$): δ = 184.36 (CH, 2 C, imine C), 159.04 (C_q, 2 C, Py C-2), 148.36 (CH, 2 C, Py C-5), 135.35 (CH, 2 C, Py C-4), 122.39 (CH, 2 C, Py C-3), 120.27 (CH, 2 C, Py C-5), 40.72 and 40.82 (CH_2, 2 C, imine-CH_2), 38.79 (CH_2, 2 C, Py-CH_2), 29.49 (CH_2, 2 C, aldehyde-CH_2), 28.68 (CH_2, 2 C, aldehyde-CH_2-CH_2) ppm; $C_{20}H_{26}N_4$ (322.45); calcd. C 74.50, H 8.13, N 17.38; found C 74.32, H 8.27, N 16.91.

[$Cu_2L_{py}2(CH_3CN)_4$](PF$_6$)$_2$ ($Cu_2L_{py}2$): Under Schlenk conditions, a solution of tetrakis(acetonitrile)copper(I) hexafluorophosphate (187 mg, 504 µmol) in acetonitrile (10 mL) was added dropwise to a solution of $L_{py}2$ (85.6 mg, 255 µmol) in acetonitrile (10 mL) and the mixture was stirred for 30 min at room temperature. The resulting residue was collected by filtration trough a Schlenk frit and dried under reduced pressure to give a light-brown solid, yield 185 mg (79%); ^{1}H NMR (400 MHz, $CDCl_3$): δ = 8.47 (br. s, 2 H, Py H-6), 7.95 (t, 2 H, Py H-4), 7.55–7.42 (m, 6 H, imine H, Py H-3, Py H-5), 3.73 (br. s, 4 H, Py-CH_2-CH_2), 3.28 (br. s, 4 H, Py-CH_2), 2.24 (s, 12 H, CH_3CN), 2.05 (br. s, 4 H, imine-CH_2), 1.25 (br. s, 4 H, imine-CH_2-CH_2) ppm. ^{13}C NMR (100 MHz, $CDCl_3$): δ = 183.99 (CH, 2 C, imine C), 160.42 (C_q, 2 C, Py C-2), 149.07 (CH, 2 C, Py C-5), 139.10 (CH, 2 C, Py C-4), 124.98 (CH, 2 C, Py C-3), 123.19 (CH, 2 C, Py C-5), 119.90 (C_q, 2 C, CN), 67.17 (CH_2, 2 C, imine-CH_2), 50.38 (CH_2, 2 C, Py-CH_2), 37.21 (CH_2, 2 C, aldehyde-CH_2), 25.27 (CH_2, 2 C, aldehyde-CH_2-*C*H_2), 0.83 (CH_3, 2 C, *C*H_3CN) ppm.$C_{28}H_{38}Cu_2F_{12}N_8P_2$ (903.68): calcd. C 37.21, H 4.24, N 12.40; found C 37.03, H 4.37, N 12.49.

[$Cu_2L_{py}2(DTBP)_2(NEt_3)_2$]·2 $NaPF_6$ (2): A solution of triethylamine (22.3 mg, 220 µmol) and Na-DTBP (50.3 mg, 220 µmol) in dichloromethane (15 mL) was added under Schlenk conditions to a solution of $Cu_2L_{py}2$ (95.0 mg, 110 µmol) in dichloromethane (10 mL). The reaction mixture was stirred under nitrogen for 30 min at room temperature. The resulting residue was collected by filtration trough a Schlenk frit und dried under reduced pressure to obtain a brown solid, yield 90 mg (58%). ^{1}H NMR (400 MHz, $CDCl_3$): δ = 8.28 (d, 2 H, *Py H-6*), 8.01 (br. s, 2 H, imine H), 7.86 (t, 2 H, *Py H-4*), 7.49 (d, 2 H, *Py H-3*), 7.32 (m, 2 H, *Py H-5*), 7.23 (d, 2 H, dtbp H-3), 6.99 (dd, 2 H, dtbp H-5), 6.71 (d, 2 H, dtbp H-6), 3.80 (t, 4 H, Py-CH_2-CH_2), 3.59 (m, 8 H, Py-CH_2, imine-CH_2), 3.28 (m, 4 H, imine-CH_2-CH_2), 3.45 (q, 12 H, triethylamine CH_2), 1.75 (m, 18 H, triethylamine CH_3) ppm.

[$Cu_2L_{py}2(OH)_2$](ClO_4)$_2$ ($CuL_{py}2$-OH): Under Schlenk conditions, a light-blue solution of copper(II)perchlorate hexahydrate (140 mg, 387 µmol) in methanol (3 mL) was added dropwise to a solution of $L_{py}2$ (61.0 mg, 189 µmol) in methanol (3 mL) and the mixture was stirred for 30 min at room temperature. The reaction mixture became dark-green and was overlaid with diethyl ether (30 mL) and allowed to stand for 2 d at 5 °C. The precipitated light-brown solid was filtered off and discarded. The filtrate was concentrated completely under reduced pressure to obtain a dark-green solid, yield 130 mg (100%). UV/Vis (acetone, 10 mm): λ_{max} (ε, L·mol^{-1}·cm^{-1}) = 364, 405, 611 (72) nm. HRMS (ESI; CH_2Cl_2, CH_3OH): *m*/*z* calcd for $C_{20}H_{30}Cu_2N_4O_2$ $[M + 2H]^+$ 484.096; found: 484.093 (intensity: 3.18·10^7); $C_{20}H_{28}Cl_2Cu_2N_4O_{10}$ (682.46): calcd. C 35.20, H 4.14, N 8.21, Cl 10.39; found C 35.03, H 4.37, N 7.79, Cl 9.95.

Stoichiometric Oxygenation of $Cu_2L_{py}2$ with the Substrate DTBP-H: A solution of $Cu_2L_{py}2$ (250 µM) was prepared under a nitrogen atmosphere by dilution of $Cu_2L_{py}2$ (5.65 mg, 6.25 µmol) in dichloromethane (25 mL). An aliquot (3 mL) of this solution was taken and placed in a cuvette (10 mm) and a UV/Vis spectrum was measured (Figure 4, black line). The remaining solution contained 4.97 mg (5.50 µmol) of $Cu_2L_{py}2$ in 22 mL of dichloromethane. To this solution was added triethylamine (11.1 mg, 11.0 µmol) and Na-DTBP (2.51 mg, 11.0 µmol) under a nitrogen atmosphere, and an aliquot (3 mL) was again placed in a cuvette (10 mm) and a UV/Vis spectrum was measured (Figure 4, green line). Molecular oxygen was then introduced into the remaining solution (19 mL) and, after 30 min, another UV/Vis spectrum was recorded (Figure 4, blue line). Subsequently, the catalytic conditions were re-established by addition of DTBP-H (98.0 mg, 475 µmol) and NEt_3 (96.1 mg, 950 µmol), followed by further oxygenation. After 60 min, a UV/Vis spectrum was measured (Figure 4, red line).

Stoichiometric Oxygenation of $Cu_2L_{py}2$ with the Substrate MeBA-OH: A solution of $Cu_2L_{py}2$ (250 µM) was prepared under a nitrogen atmosphere by dilution of $Cu_2L_{py}2$ (5.65 mg, 6.25 µmol) in dichloromethane (25 mL). An aliquot (3 mL) of this solution was taken and placed in a cuvette (10 mm) and a UV/Vis spectrum was measured (Figure 5, black line). The remaining solution contained 4.97 mg (5.50 µmol) of $Cu_2L_{py}2$ in 22 mL of dichloromethane. To this solution was added triethylamine (22.2 mg, 22.0 µmol) and MeBA-OH (1.67 mg, 11.0 µmol) under a nitrogen atmosphere, and an aliquot (3 mL) was again placed in a cuvette (10 mm) and a UV/Vis spectrum was measured (Figure 5, green line). Molecular oxygen was then introduced into the remaining solution (19 mL) and, after 30 min, another UV/Vis spectrum was recorded (Figure 5, blue line). Subsequently, the catalytic conditions were re-established by addition of MeBA-OH (72.3 mg, 475 µmol) and NEt_3 (96.1 mg, 950 µmol), followed by further oxygenation. After 60 min, a UV/Vis spectrum was measured (Figure 5, red line).

Kinetic Measurements: Concentration dependence of the Catalyst $Cu_2L_{py}2$ on the product formation was measured as follows. Solutions with different concentrations of $Cu_2L_{py}2$ in dichloromethane (10 mL) were prepared under a nitrogen atmosphere (500, 250, 125, and 50 µM). A mixture of DTBP-H (100 equiv.) and triethylamine (200 equiv.) was added to each of the solutions with different concentrations of $Cu_2L_{py}2$ in dichloromethane under anaerobic conditions, and then molecular oxygen was bubbled through the solution. The catalytic formation of DTBQ was detected by the evolution of the 407 nm absorption band by recording UV/Vis spectroscopy during the first 15 min of oxygenation (see the Supporting Information, Figure S1).

Acknowledgments

The authors would like to thank Prof. Dr. J. Grotemeyer for the mass spectrometric measurements. The authors also thank the Deutsche Forschungsgemeinschaft (DFG), CAU Kiel, and COST CM1003 for financial support of this research.

[1] G. Prota, *Med. Res. Rev.* **1988**, *8*, 525.
[2] A. Sánchez-Ferrer, J. N. Rodríguez-López, F. García-Cánovas, F. García-Carmona, *Biochim. Biophys. Acta* **1995**, *1247*, 1.
[3] a) H. S. Raper, *Biochem. J.* **1927**, *21*, 89; b) H. S. Raper, E. J. Wayne, *Biochem. J.* **1928**, *22*, 188; c) K. T. Yasunobu, E. W. Peterson, H. S. Mason, *J. Biol. Chem.* **1959**, *234*, 3291.
[4] M. E. Cuff, K. I. Miller, K. E. van Holde, W. A. Hendrickson, *J. Mol. Biol.* **1998**, *278*, 855.
[5] M. Rolff, J. Schottenheim, H. Decker, F. Tuczek, *Chem. Soc. Rev.* **2011**, *40*, 4077.

[6] C. Gerdemann, C. Eicken, B. Krebs, *Acc. Chem. Res.* **2002**, *35*, 183.
[7] Y. Matoba, T. Kumagai, A. Yamamoto, H. Yoshitsu, M. Sugiyama, *J. Biol. Chem.* **2006**, *281*, 8981.
[8] H. Decker, T. Schweikardt, F. Tuczek, *Angew. Chem. Int. Ed.* **2006**, *45*, 4546; *Angew. Chem.* **2006**, *118*, 4658.
[9] Y. Li, Y. Wang, H. Jiang, J. Deng, *Proc. Natl. Acad. Sci. USA* **2009**, *106*, 17002.
[10] a) W. T. Ismaya, H. J. Rozeboom, A. Weijn, J. J. Mes, F. Fusetti, H. J. Wichers, B. W. Dijkstra, *Biochemistry* **2011**, *50*, 5477; b) M. Sendovski, M. Kanteev, V. S. Ben-Yosef, N. Adir, A. Fishman, *J. Mol. Biol.* **2011**, *405*, 227; c) M. Goldfeder, M. Kanteev, S. Isaschar-Ovdat, N. Adir, A. Fishman, *Nat. Commun.* **2014**, *5*, 4505.
[11] a) E. A. Lewis, W. B. Tolman, *Chem. Rev.* **2004**, *104*, 1047; b) L. M. Mirica, X. Ottenwaelder, T. D. P. Stack, *Chem. Rev.* **2004**, *104*, 1013; c) I. A. Koval, P. Gamez, C. Belle, K. Selmeczi, J. Reedijk, *Chem. Soc. Rev.* **2006**, *35*, 814.
[12] J. E. Bulkowski, *United States Patent* 4.545.937 **1985**, *Oct. 8*.
[13] M. Réglier, C. Jorand, B. J. Waegell, *Chem. Soc. Chem. Commun.* **1990**, 1752.
[14] L. Casella, M. Gullotti, R. Radaelli, P. J. Digennaro, *Chem. Soc. Chem. Commun.* **1991**, 1611.
[15] M. Rolff, J. Schottenheim, G. Peters, F. Tuczek, *Angew. Chem. Int. Ed.* **2010**, *49*, 6438; *Angew. Chem.* **2010**, *122*, 6583.
[16] J. Schottenheim, N. Fateeva, W. Thimm, J. Krahmer, F. Tuczek, *Z. Anorg. Allg. Chem.* **2013**, *639*, 1491.
[17] J. N. Hamann, F. Tuczek, *Chem. Commun.* **2014**, *50*, 2298.
[18] A. Hoffmann, C. Citek, S. Binder, A. Goos, M. O. Rübhausen, O. Troeppner, I. Ivanovic-Burmazovic, E. C. Wasinger, T. D. P. Stack, S. Herres-Pawlis, *Angew. Chem. Int. Ed.* **2013**, *52*, 5398; *Angew. Chem.* **2013**, *125*, 5508.
[19] a) C. M. Binder, D. D. Dixon, E. Almaraz, M. A. Tius, B. Singaram, *Tetrahedron Lett.* **2008**, *49*, 2764; b) The synthesis was varied.
[20] G. J. H. Buisman, P. C. J. Kamer, P. W. N. M. van Leeuwen, *Tetrahedron: Asymmetry* **1993**, *4*, 1625.
[21] P. Capdevielle, M. Maumy, *Tetrahedron Lett.* **1982**, *23*, 1573.
[22] a) K. D. Karlin, Z. Tyeklar, A. Farooq, M. S. Haka, P. Ghosh, R. W. Cruse, Y. Gultneh, J. C. Hayes, P. J. Toscano, J. Zubieta, *Inorg. Chem.* **1992**, *31*, 1436; b) H.-C. Liang, K. D. Karlin, R. Dyson, S. Kaderli, B. Jung, A. D. Zuberbuehler, *Inorg. Chem.* **2000**, *39*, 5884; c) T. Matsumoto, H. Furutachi, S. Nagatomo, T. Tosha, S. Fujinami, T. Kitagawa, M. Suzuki, *J. Organomet. Chem.* **2007**, *692*, 111.
[23] M. D. Stallings, M. M. Morrison, D. T. Sawyer, *Inorg. Chem.* **1981**, *20*, 2655.
[24] S. Harmalker, S. E. Jones, D. T. Sawyer, *Inorg. Chem.* **1983**, *22*, 2790.
[25] K. D. Karlin, M. S. Nasir, B. I. Cohen, R. W. Cruse, S. Kaderli, A. D. Zuberbühler, *J. Am. Chem. Soc.* **1994**, *116*, 1324.
[26] L. Casella, E. Monzani, *Inorg. Chem.* **1996**, *35*, 7516.
[27] E. Peyroux, W. Ghattas, R. Hardré, M. Giorgi, B. Faure, A. J. Simaan, C. Belle, M. Réglier, *Inorg. Chem.* **2009**, *48*, 10874.
[28] C. Bochot, A. Gouron, L. Bubacco, A. Milet, C. Philouze, M. Reglier, G. Serratrice, H. Jamet, C. Belle, *Chem. Commun.* **2014**, *50*, 308.
[29] a) C. Arcus, K. Fivizzani, S. F. Pavkovic, *J. Inorg. Nucl. Chem.* **1977**, *39*, 285; b) The synthesis was varied.
[30] M. Kodera, T. Kawata, K. Kano, Y. Tachi, S. Itoh, S. Kojo, *Bull. Chem. Soc. Jpn.* **2003**, *76*, 1957.
[31] J. S. Thompson, J. C. Calabrese, *Inorg. Chem.* **1985**, *24*, 3167.
[32] P. Verma, J. Weir, L. Meirica, T. D. P. Stack, *Inorg. Chem.* **2011**, *50*, 9816.
[33] J. Rall, M. Wanner, M. Albrecht, F. M. Hornung, W. Kaim, *Chem. Eur. J.* **1999**, *5*, 2802.
[34] W. Kaim, B. Schwederski, *Coord. Chem. Rev.* **2010**, *254*, 1580.
[35] a) G. Battaini, M. De Carolis, E. Monzani, F. Tuczek, L. Casella, *Chem. Commun.* **2003**, 726; b) L. Santagostini, M. Gullotti, E. Monzani, L. Casella, R. Dillinger, F. Tuczek, *Chem. Eur. J.* **2000**, *6*, 519.
[36] W. Schöniger, *Microchim. Acta* **1955**, *43*, 123.

Received: January 13, 2015
Published Online: ■

EurJIC European Journal of Inorganic Chemistry

Tyrosinase Models

Keywords: Bioinorganic chemistry / Metalloproteins / Enzyme models / Enzyme catalysis / Copper

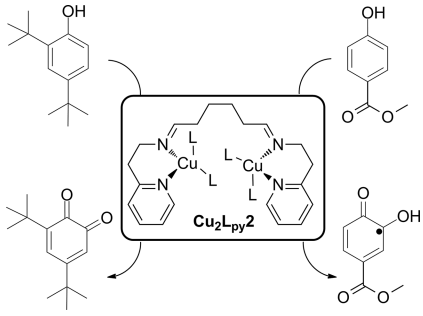

A tyrosinase model based on the binucleating ligand $L_{py}2$ was developed and characterized. The ligand $L_{py}2$ contains a combination of an imine and a pyridine function in the sidearms that are bridged by a flexible alkyl spacer. The $Cu_2L_{py}2$ complex catalyzes the conversion of monophenol DTBP-H into the *o*-quinone DTBQ (TON = 18). An electron-poor substrate is converted into the semiquinone.

